

# PHOENICS Newsletter



**CHAM**



Table of Contents	
Page	
2	What's New in PHOENICS 2025
3	PHOENICS Implementation of the Spalart-Allmaras Turbulence Model
6	Damping of Internal Waves at Boundaries
9	ZW3D Flow: An Embedded CFD Tool Tailored for Designers
10	PHOENICS Showcases Cutting-Edge CFD Capabilities at Hannover Messe 2025
12	CHAM Announces the Retirement of One of its Long-Standing Employees and Contact Us

Concentration, Heat and Momentum Limited (CHAM)

Bakery House, 40 High Street, Wimbledon Village, London, SW19 5AU, England

Tel: +44 (0)20 8947 7651 Email: [phoenics@cham.co.uk](mailto:phoenics@cham.co.uk) Web: [www.cham.co.uk](http://www.cham.co.uk)

Summer  
2025

# What's New in PHOENICS 2025

*Dr Timothy Brauner, R&D Manager, CHAM*

## Introduction

The latest version of PHOENICS is here: PHOENICS 2025 version 1.0. It brings with it additions and improvements to the VR-Editor, VR-Viewer, the Earth Solver and also to Unstructured PHOENICS (USP). These updates provide expanded physical-modelling capabilities, improved usability, and bring USP closer to leaving beta-status, as well as corrections and fixes across PHOENICS. Some features are highlighted below, for the full list please see **TR006 – What's New in PHOENICS**.

## Earth Solver

PHOENICS now provides access to the Spalart-Allmaras (SA) one-equation turbulence model. Designed for aerodynamic and wall-bounded flow simulations, the model is offered in both high- and low-Reynolds-number forms. It is compatible with Cartesian, polar, and body-fitted coordinate meshes and works with both SPARSOL and PARSOL. Although originally developed for external aerodynamic flows, the SA model offers a good balance of accuracy and computational efficiency across a wide range of applications. Example cases are included in the PHOENICS Input Library, and a complete technical description is available in POLIS.

The Volume of Fluid (VOF) method now supports a two-phase evaporation, boiling, and condensation mechanism. The implementation distinguishes between film and bulk boiling through separate evaporation-rate formulations. The model uses a non-conservative form of the VOF equation, assumes incompressible fluids, and includes a revised energy-equation formulation to account for latent heat effects.

The VOF method also receives an additional surface tension model, “second-order-in-temperature”, which addresses cases where a linear relationship between temperature and surface tension is insufficient. VOF may benefit from this in simulations involving thermo-capillary or Marangoni forces.

PHOENICS' Non-Newtonian fluid-modelling capabilities have been extended with a modified power-law viscosity, which was used in simulations for the turbulent pipe flow of a pseudo-plastic fluid.

## VR-Editor & VR-Viewer

The VR-Editor now has two new options for specifying turbulence boundary conditions at inlets: In addition to the two existing modes, 'Intensity + Auto Length Scale' and 'User Set', two new types are now available: 'Intensity + Viscosity Ratio' and 'Intensity + Length Scale'. The new

'Viscosity Ratio' option calculates inlet conditions based on turbulence intensity and the ratio of turbulent to laminar viscosity, and the new 'Length Scale' option allows the user to specify the Prandtl's mixing length directly in conjunction with turbulence intensity.

To facilitate before and after comparisons and scenario testing, a new toggle switch has been added to the Object Specification dialog. This feature allows users to deactivate objects without removing them or altering their type, preventing any unwanted impact on the computational grid and simplifying workflow during testing and setup.

Amongst others, conveniences added include line plotting at cell centres along constant I, J, or K directions, access to storage of quantities such as the dynamic turbulent viscosity, or additional output from body force integration.

## Unstructured PHOENICS (USP) (beta)

Work on USP has continued and it receives several expansions to its capabilities.

USP takes the standard PHOENICS Cartesian grid and adds levels of grid refinement close to items of interest. Users can now view the USP grid in the VR-Editor, with a new toggle option added under the Mesh menu to switch between the USP and original Cartesian grids. This addition should facilitate grid set up.

USP's grid is generated by a special utility called USPGRID, which has been reworked significantly: from changes to data structures, updates to algorithms, and data output to support new features. Additionally, to improve geometric flexibility, support for Angled-In and Angled-Out objects has been added to USP.

Lastly, but not least, USP can now run Hydrodynamics simulations in parallel thanks to an expansion of the code, as well as the new PAR\_USP tool, which partitions the USP mesh for parallel execution.

USP is under development and is still in “beta” status i.e. it still contains some deficiencies and issues.

## Corrections

In addition to the above highlighted features, PHOENICS has also received numerous improvements and corrections. These range from extended multi-byte character support, upgrades to FLAIR, e.g. the option to include humidity in the calculation of mixture density, upgrades to plotting cut-cells and double-cut cells, and improvements to robustness in

respect of updated solver settings and boundary treatments for IMMERSOL, and the turbulence generation term, to name a few.

For the full list of additions and corrections please see TR006 – What’s New in PHOENICS.

# PHOENICS Implementation of the Spalart-Allmaras Turbulence Model

*Kathryn Kleijn, CFD Engineer, CHAM*

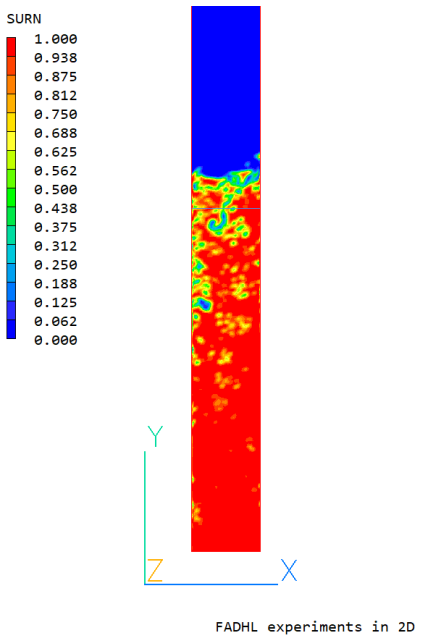


**Fig.1 VOF: - Evaporation and Condensation in a Closed Thermosyphon**

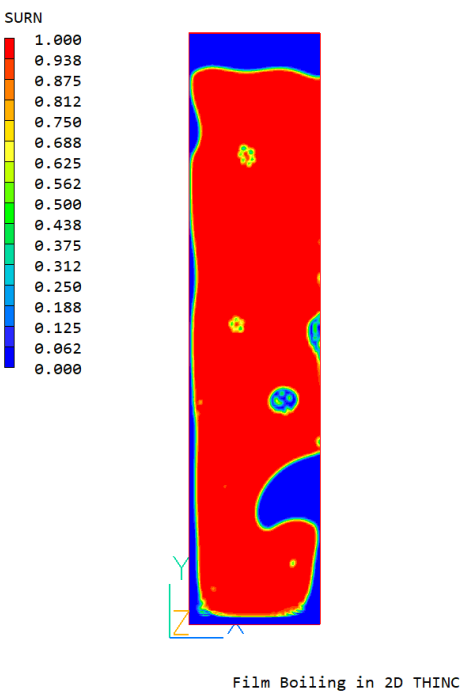


**Fig 2 VOF: - Film Boiling in an Open Container**

## 1. Introduction

The Spalart-Allmaras (SA) model is a one-equation turbulence model designed for aerodynamic applications involving wall-bounded flows. First introduced in 1992 [1], it is a low-Reynolds number (LRN) model that solves for the undamped turbulent kinematic viscosity. Whilst it has been calibrated and widely used for wall-bounded aerodynamic and turbomachinery applications, it is unable to model free shear flows and decaying turbulence with accuracy.

Its main advantage is its simplicity, requiring less computation time than more complex 2-equation models. The model is also considered more robust than the LRN k-ε model, providing reasonable results on relatively coarse grids compared to the finer grids required by more complex LRN models. However, this simplicity means that in some flows, accuracy is lost compared to the 2-equation models.

Although designed as a LRN model, the SA model can be adapted for use with wall functions in a high Reynolds-number closure. In addition, a number of variants of the original model have been proposed, such as modifications to account for rotation and curvature effects, and handling negative viscosity values. A full list of the variations with detailed descriptions can be found at [2]. These modifications can be applied individually or in combinations to the original model.

This article reports on the provision of the SA turbulence model as a standard option in PHOENICS Classic 2025. The motivation for including this model in PHOENICS stems not only from its popularity, but also from its ability to provide cost-effective solutions for wall-bounded flows. The remainder of this article provides brief details on the implementation, activation, verification and validation of the model. Some concluding remarks are provided in section 4.

## 2. The PHOENICS CFD Model

In PHOENICS, the SA model is implemented without any trip terms, which follows standard practice. The original model includes two trip terms, but both are generally omitted, which assumes the presence of free-stream turbulence. A rotation correction [3] is included in the production term of the undamped turbulent kinematic viscosity, with a lower limit [2] imposed to avoid the numerical problems which would arise if the term became zero or negative. The rotation correction reduces eddy viscosity in regions where vorticity exceeds strain rate. The model is available in both high- and low-Reynolds number forms within PHOENICS.

The high-Reynolds number model uses equilibrium wall functions and the value of the undamped turbulent kinematic viscosity at the wall is dependent on the friction velocity. The LRN model integrates down to the wall with zero turbulent kinematic viscosity at the wall, requiring  $y^+$  values near 1.

The SA model has been implemented for Cartesian, polar and BFC meshes, and can be used with both SPARSOL and PARSOL. Users can activate the model from the VR menu, in *Main Menu > Models > Turbulence models*. The options for the high- and low-Reynolds number models are selected as “Spalart-Allmaras” and “Spal-Allm-lowRe” respectively (Figure 1). The undamped turbulent kinematic viscosity is stored as ENTI with default whole-field solution.

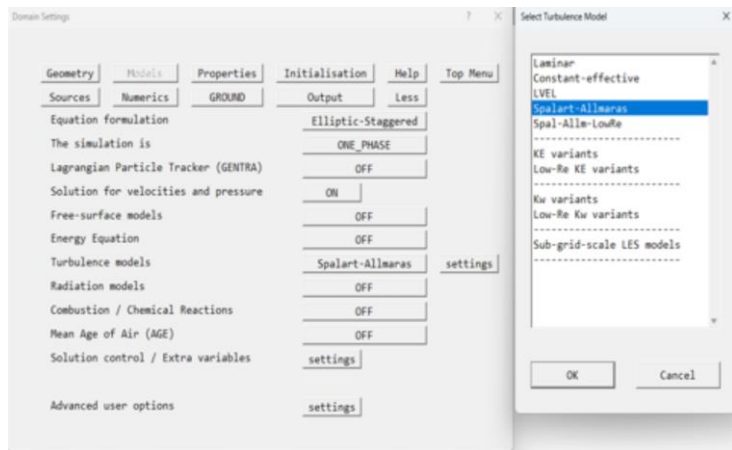


Figure 1 - VR Menu selection

The model has been tested on the Stones solver in serial and on the default parallel solver in PHOENICS. Convergence is generally good provided near-wall velocity values remain stable. It is recommended to apply linear relaxation to ENTI, with values of 0.3-0.5 giving good convergence during model verification and validation.

Several example cases are included in the PHOENICS library (see Applications section), and a full technical description is included in POLIS at:

[https://www.cham.co.uk/phoenics/d\\_polis/d\\_enc/turmod/enc\\_t322.htm](https://www.cham.co.uk/phoenics/d_polis/d_enc/turmod/enc_t322.htm)

### 3. Applications

This section will present the validation cases and 3D time comparisons to demonstrate the advantages of the SA model over the more complex 2-equation models.

#### 3.1. Validation

The model has been successfully validated in PHOENICS for a selection of cases, including channel and pipe flow, flow past a backward-facing step, flow over a flat plate, flow past a blunt flat plate and flow over a surface-mounted square rib. Additional cases for aerofoils and 3D flow past a surface-

mounted cube have been validated for the high-Reynolds number form of the model. Due to time constraints, these cases have not included grid-sensitivity studies.

The results for flow over a flat plate, flow over a backward-facing step and flow past a blunt flat plate will be presented here.

**Flow over a Flat Plate:** The problem considered is steady, incompressible, turbulent flow across a smooth flat plate with zero pressure gradient. Since this is one of the cases on which the original model was calibrated, we would expect the SA model predictions to be in strong agreement with the expected values, and this is the case for all predicted quantities. Figure 2 shows the predicted  $u^+$  profile near the wall compared to theoretical values. The PHOENICS prediction shows excellent agreement. Additionally, Figure 3 shows the predicted skin friction coefficient compared to the correlation of Schlichting [5], again showing excellent agreement.

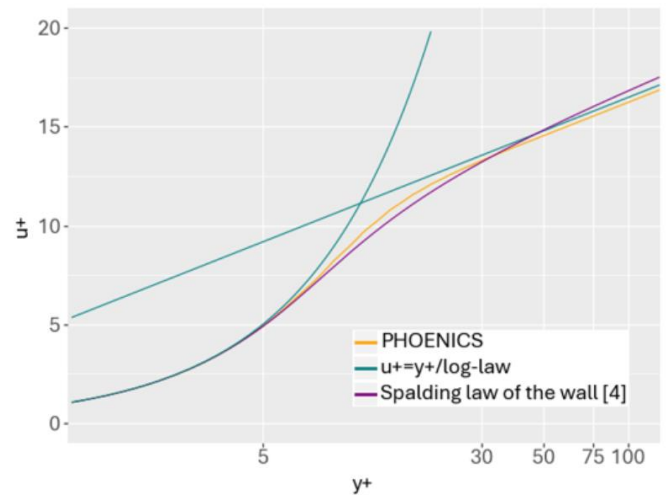


Figure 2 - Flow along a flat plate,  $u^+$  profile

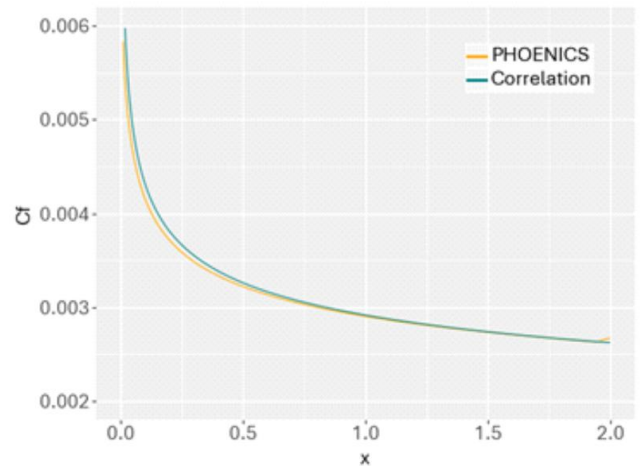
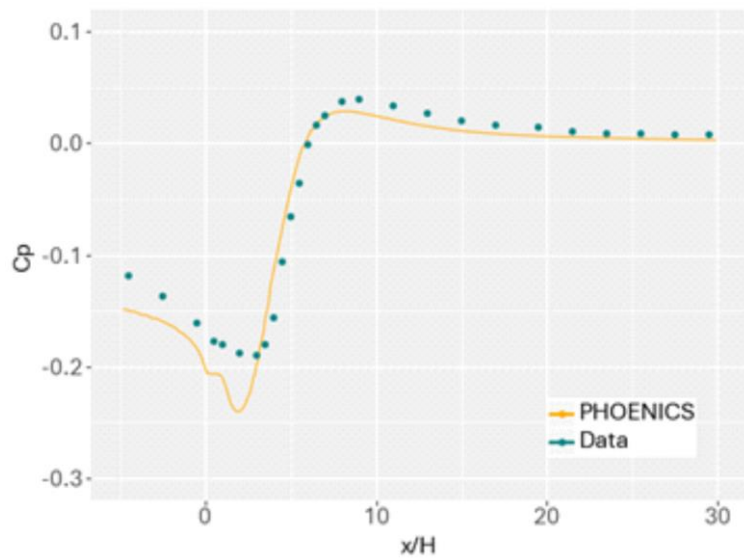


Figure 3 - Skin friction coefficient along a flat plate

**Backward-facing step:** This case is 2D flow over a backward facing step in a channel, with an expansion ratio of 1.125, and Reynolds number of 36,000 based on step height  $H$ . The SA model captures the separation region well, predicting a reattachment length  $x/H$  of 6.4 and 6.0 in the low- and high-Reynolds cases respectively, in good agreement with experimental results of 6.26. Figure 4 shows the pressure coefficient compared to the data of Driver and Seegmiller [6], again demonstrating good agreement.



**Figure 4 - Pressure coefficient over a backward-facing step**

**Flow past a Blunt Flat Plate:** The case considered is 2D, incompressible, turbulent flow past a thick flat rectangular plate with a sharp leading edge, with Reynolds number 50,000 based on plate thickness  $H$ . The flow separates at the leading edge of the plate, forming a long separation zone over the top of the plate, which reattaches further downstream. The SA model predicts a reattachment length  $x/H$  of 4.8 and 4.5 for the low- and high-Reynolds number models respectively, consistent with the experimental result of 4.7. Figure 5 shows the velocity contours and filtered vectors around the separation zone on top of the plate.

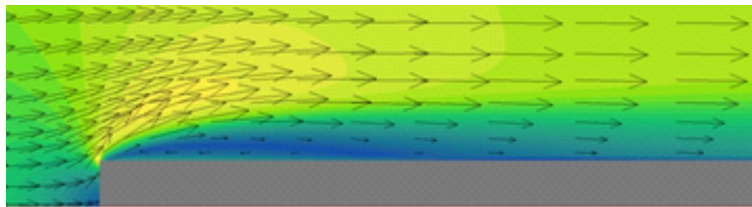


**Figure 5 - Velocity contours and filtered vectors over a blunt flat plate**

### 3.2. 3D Time Comparison

A selection of 3D cases have been run in order to compare the computer time needed for the SA model with that required for more complex 2-equation models.

The first comparison is for a steady case using the high-Reynolds closure of the SA model. This was run for an aerofoil, and compared to the Chen-Kim  $k-\epsilon$  model. The SA model gave around a 30% decrease in computer time compared to the Chen-Kim  $k-\epsilon$  model. Both models gave very similar results, with predicted lift and drag coefficients in agreement.

A steady electronics-cooling case was run, using the low-Reynolds form of the SA. This was done in comparison to the two-layer  $k-\epsilon$  model. The SA model showed superior convergence over the two-layer model, with a saving of approximately 70% computer time. The accuracy of the SA model in this case was compromised, because the electronics-cooling case involved circular inlets, which produced jets. The SA model showed increased spreading of these jets, as expected since the model is not designed for this type of flow, leading to higher temperature predictions. However, the computer savings show the potential for this model in other electronics-cooling applications.

Finally, a comparison between SA and the Chen-Kim  $k-\epsilon$  model was conducted for a transient case. This case was the flow past a surface-mounted cube, using the high-Reynolds form. Both models gave similar results, with the SA model predicting a slightly shorter (and more accurate) separation length. The SA model also gave savings of over 50% computer time compared to the Chen-Kim  $k-\epsilon$  model.

These results show that the SA model gives significant savings in computer time compared to more complex models, especially for transient cases and in the low-Reynolds form, with convergence more easily procured in the low-Reynolds form than with other models.

## 4. Conclusion

The SA turbulence model has been successfully implemented into the PHOENICS code in high- and low-Reynolds-number forms, both of which can be activated from the VR menu. It is available for Cartesian, polar and BFC meshes, and can be used with both SPARSOL and PARSOL. The implementation has been validated for a number of cases, with results showing good agreement with expectations. The SA model was initially designed for external flows, and as such performs especially well in these cases. Its computational efficiency and robustness make it a good choice for many applications, although it may sacrifice some accuracy relative to more complex two-equation models. Caution is advised when using the SA model for untested industrial applications, and in flows with free shear and decaying turbulence, such as jets where the model is known to be unsuitable. With the model now available for use with equilibrium wall functions and integration down to the wall, future work will investigate the use of an automatic wall treatment to make the solution less sensitive to near-wall mesh refinement

## 5. References

[1] Spalart, P.R. & Allmaras, S.R. (1992). "A One-Equation Turbulence Model for Aerodynamic Flows" AIAA-92-0439

[2] NASA. *The Spalart-Allmaras Turbulence Model*.

<https://turbmodels.larc.nasa.gov/spalart.html>. [Accessed 6th May 2025]

[3] Dacles-Mariani, J., Zilliac, G. G., Chow, J. S., and Bradshaw, P. Numerical/Experimental Study of a Wingtip Vortex in the Near Field. *AIAA Journal*. 1995; 33(9):1561-1568.

<https://doi.org/10.2514/3.12826>

[4] Spalding, D.B. A Single Formula for the "Law of the Wall". *J. Appl. Mech.* Sep 1961; 28(3):455-458.

<https://doi.org/10.1115/1.3641728>

[5] Schlichting, H. *Boundary Layer Theory*. 6<sup>th</sup> ed. New York: McGraw Hill; 1968

[6] Driver, D. M. and Seegmiller, H. L. Features of Reattaching Turbulent Shear Layer in Divergent Channel Flow. *AIAA Journal*. 1985; 23(2):163-171.

<https://doi.org/10.2514/3.8890>

## Damping of Internal Waves at Boundaries

*Dr. R. P. Hornby (Retired Research Engineer,  
ex DSTL, DERA & NNC)*

### 1. Introduction

When simulating the wave motion of a fluid, problems can be caused by waves reflected at the domain boundaries, particularly if these waves do not form part of the required simulation. Various techniques have been employed to minimise the effect of such reflected waves on flow simulations [1]. In principle the domain can be extended to distances such that any reflections are sufficiently weak, but this is computationally expensive. The most popular methods employ a sponge layer along the boundaries with resistive source terms in the momentum equations designed to absorb the incoming wave energy. This article illustrates the use of such methods in PHOENICS simulations of internal wave flows, but these methods are equally useful for other wave motions.

### 2. Analysis

For simplicity, a 2-D time-dependent analysis is carried out for a body vibrating in a uniformly stratified environment. PHOENICS is used to solve the time-dependent laminar equations of mass, momentum and energy. A Cartesian grid is used with the KOREN differencing scheme. The  $x$ ,  $y$  and  $z$  coordinates are taken in the lateral and vertical directions respectively, with the  $z$  coordinate in the direction of oscillation. The local buoyancy frequency is given by

$$N = \text{sqrt}\left(-g \frac{d\rho}{\rho dz}\right) \quad (1)$$

where  $g$  is the acceleration due to gravity and  $\rho$  the density.  $N$  is a constant. For a vibrating body, waves of frequency less than  $N$  [2] will be found in directions to the vertical, where

$$\cos(\theta) = \frac{\omega}{N} \quad (2)$$

To explore damping of the waves at the domain boundary, a sponge layer is included along the top and bottom boundaries (where the wave reflections would otherwise take place). In this sponge layer, linear or quadratic resistive source terms can be employed or a combination of both. Alternatively, enhancement of the fluid viscosity in the sponge layer would be expected to achieve a similar result.

A linear resistive source term per unit volume would take the form

$$SL = -\rho\alpha\omega\gamma U \quad (3)$$

where  $U$  is the vertical or horizontal component of velocity and a quadratic resistive source term per unit volume would have the form

$$SQ = -\rho\beta k\gamma U[U] \quad (4)$$

where  $\alpha$  and  $\beta$  are positive non-dimensional constants,  $k$  is the wavenumber and  $\gamma$  is a blending function which increases gradually from zero to one into the sponge layer.

A suitable blending function given in [1] is

$$\gamma = \frac{(e^s - 1)}{(e - 1)} \quad (5)$$

where

$$s = \left(\frac{Z}{L}\right)^n \quad (6)$$

$z$  is the distance into the sponge layer of thickness  $L$  and  $n$  is a constant which controls the degree of blending (usually 1,2 or 4) with higher values of  $n$  producing more gradual damping with distance.

For viscosity damping, the laminar kinematic viscosity in the momentum equations for the sponge layer is taken as

$$(1 + \gamma f)\nu \quad (7)$$

where  $f$  is a non-dimensional viscosity-enhancement factor and  $\nu$  is the laminar kinematic viscosity outside the sponge layer. A crude estimate for  $f$  is

$$\frac{UL}{Re\nu} \quad (8)$$

where  $U$  and  $L$  are local velocity and length scales, and  $Re$  is a specified local Reynolds Number  $<1$  which implies dominance of viscous effects.

For all cases, values of  $\alpha, \beta, n$  and  $f$  require some degree of trial and error, although the former two parameters are expected to be  $O(1)$ .

### 3. Results

The simulations are required in reality over an infinite domain, but in practice only a finite domain can be modelled with a finite amount of computer time. Figure 1 shows the modelled domain filled with a fluid uniformly stratified in the vertical  $z$  direction. Illustrative results using the above analysis are shown in Figure 1.

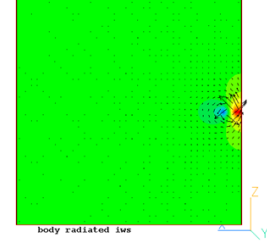


**Figure 1. 2-D domain for internal-wave damping simulations. The vibrating body is shown placed mid-way down the right hand side of the domain.**

using a vertically vibrating sinusoidal source of wave frequency,  $\omega$  placed mid-way down the boundary of the domain.

The value of  $\omega$  is taken to produce a beam of internal waves directed at 45 degrees to the vertical with wavenumber,  $k$ , related to the size of the vibrating body. The results from this simulation are shown in Figure 2. As can be seen, the internal wave energy is channelled in beams at 45 degrees to the vertical, and is reflected at the top and bottom boundaries, and eventually at the side boundary, and then back to the source location.

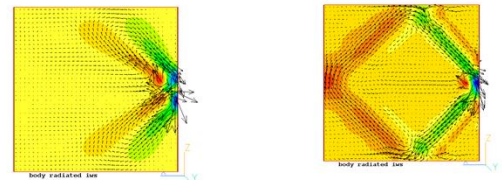


**Figure 2 (a) Left hand plot shows velocity vectors and vertical velocity contours of the internal wave beams emanating from the source and travelling towards the top and bottom boundaries. (b) This shows a later time when the internal wave beams have reached and reflected from the top, bottom and side boundaries.**

If these wave reflections are undesirable, then they need to be suppressed. This can be achieved by introducing a sponge layer at the top and bottom boundaries with widths typically of a few wavelengths. Within the sponge layer, resistive terms are included as source terms in both momentum equations, or as another option, the fluid viscosity is substantially increased. Three illustrative simulations are performed with results presented at the same time in the simulation, as in Figure 2b. In the first simulation, linear

source terms are used with  $\alpha$  equal to  $\frac{1}{2}$ . The results are shown in Figure 3. As can be seen, there is a marked reduction in reflected wave energy.

In the second simulation, Figure 4 shows equivalent results using quadratic wave damping with  $\alpha$  equal to 7. Again, there is significant reduction in the reflected wave energy.

The third simulation uses viscosity damping in the sponge layers with results similar to those obtained in simulations 2 and 3, see Figure 5

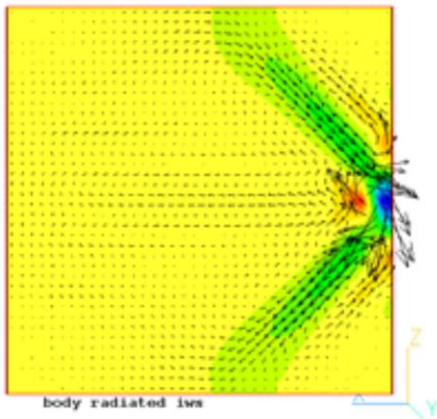


**Figure 3. Linear wave damping: velocity vectors and vertical velocity contours of the internal wave beams at the same time in the simulation as Figure 2b, showing the marked reduction in reflected wave energy ( $\alpha=1, n=1$ ).**

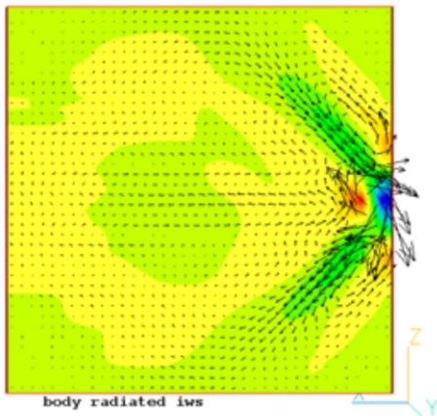


**Figure 4. Quadratic wave damping: velocity vectors and vertical velocity contours of the internal wave beams at the same time in the simulation as Figure 2b, showing the marked reduction in reflected wave energy ( $\alpha=7, n=1$ ).**

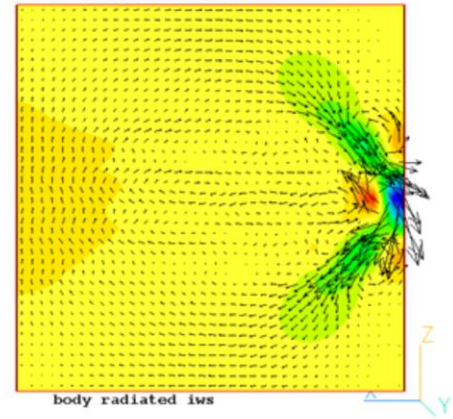


**Figure 5. Viscosity wave damping: velocity vectors and vertical velocity contours of the internal wave beams at the same time in the simulation as Figure 2b, showing the marked reduction in reflected wave energy .**

#### 4. Conclusions

It has been shown that internal wave reflection from boundaries can be substantially reduced by introducing a sponge layer incorporating linear or quadratic resistive terms in the momentum equations, or by enhancement of the fluid viscosity. The degree to which the reflected waves are damped is controlled by the non-dimensional parameters given above and some experimentation is required to determine the best choice for a particular simulation. It is expected that similar treatment will prove beneficial in reducing boundary reflection of other fluid wave types.

#### 5. References

1. Perić, R., & Abdel-Maksoud, M. (2016). Reliable damping of free-surface waves in numerical simulations. *Ship Technology Research*, 63(1), 1–13. <https://doi.org/10.1080/09377255.2015.1119921>
2. Lighthill, M.J. (1978). *Waves in fluids*. Cambridge University Press.

- Collaboration Without Barriers: Unified data sources enable cross-departmental optimization.
- Real-Time Innovation: Shifting from "post-facto correction" to "live innovation" for market agility.

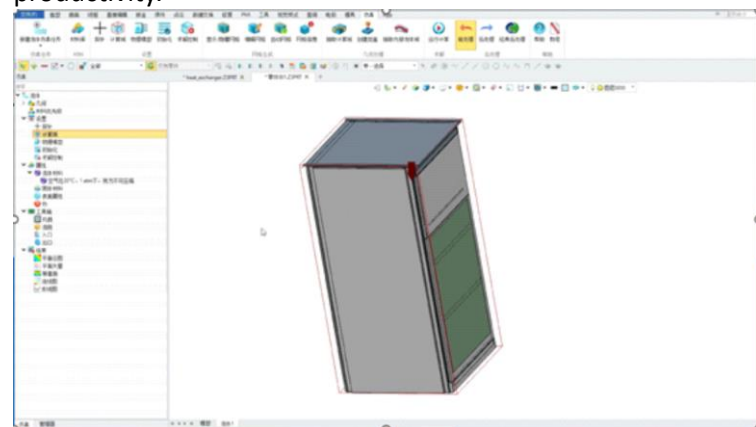
Enterprises no longer need to compromise with "high costs, low efficiency, and slow feedback." Instead, they unlock a self-reinforcing innovation cycle: "Design is Simulation, Simulation is Optimization."

### 3. ZW3D Flow: Where Design and Simulation Converge

ZW3D Flow is not merely a functional add-on but a fundamental reimagining of simulation workflows—empowering fluid/thermal designers with industrial-grade CFD capabilities within their familiar ZW3D environment.

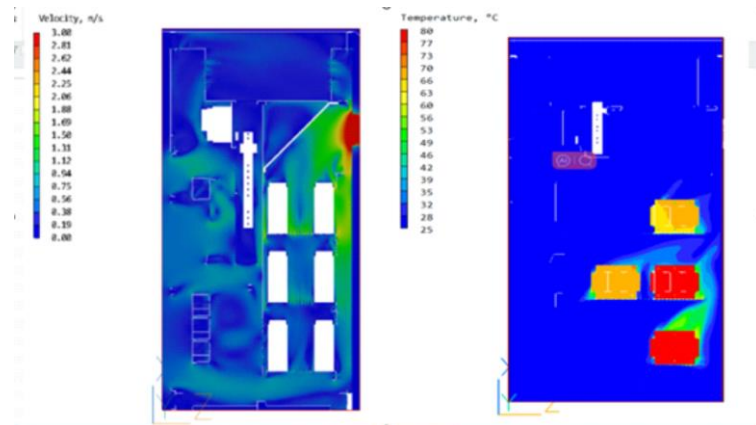
Let's consider a real case: A leading Chinese electrical switchgear producer—supplying critical power control hubs for mega-factories and substations across Western China—faced chronic project delays. Their challenge is that while structural robustness was paramount, thermal management under high-voltage operations proved the decisive performance metric.

During initial consultations, we diagnosed the core issue: Frequent thermal design modifications, driven by evolving voltage-environment requirements, forced cross-departmental negotiations between thermal engineers, structural designers, and prototyping teams. This disjointed workflow strangled productivity.



### With ZW3D Flow:

- Thermal designers directly accessed structural CAD models in ZW3D.
- Post-thermal layout adjustments, CFD validation ran instantly on the same workstation.
- Cross-team collaboration bottlenecks dissolved, **significantly reducing delivery delays.**



### 4. Empowering Design, Defining the Future with Innovation

ZW3D Flow heralds CFD's evolution from an expert-exclusive tool to a democratized design accelerator. We envision a future where: **CFD becomes as intuitive as breathing**—designers click in ZW3D, and fluid analysis results materialize in real time. The legendary PHOENICS engine transforms into an invisible intelligence hub, making complex flow insights as simple as measuring dimensions. **This is the ultimate vision of Industry 4.0: an end to the fragmented "design-then-simulate" era.**

### Call to Action

We cordially invite product designers across manufacturing industries to experience ZW3D 2026 and its CFD module, ZW3D Flow. Apply for ZW3D 2026 trial at [www.zwsoft.com](http://www.zwsoft.com)

*"Where every design decision is instantly validated, and simulation is no longer a checkpoint—but the very canvas of creation."*

## PHOENICS Showcases Cutting-Edge CFD Capabilities at Hannover Messe 2025

Dr Wenjun Tan, CAE Product Manager, ZWSOFT

HANNOVER, Germany, 23 April, 2025

PHOENICS, the flagship computational fluid dynamics (CFD) software from CHAM, took centre stage at ZWSOFT's exhibition during the prestigious Hannover Messe 2025. The world's leading industrial technology trade fair was held at the Hannover Exhibition Centre from April 21 to 25.



Marking its third consecutive year of participation since 2023, ZWSOFT significantly expanded its presence at this global platform. CHAM, a wholly-owned subsidiary of ZWSOFT and a renowned global CFD software developer, prominently featured its next-generation general-purpose CFD simulation solution, PHOENICS.

### Keynote Highlights PHOENICS' Engineering Value

Dr. Timothy Brauner, a senior technical CFD expert from CHAM, delivered a keynote address titled "Empowering the Future of Industrial Design: The Intelligent Simulation Approach of PHOENICS." He presented to an engaged audience the software's core functionalities, unique advantages, and its demonstrated excellence in solving complex industrial fluid-dynamics challenges.



Through practical case studies, Dr. Timothy Brauner illustrated PHOENICS' role in driving breakthroughs across product design, process optimization, and energy efficiency – particularly within critical sectors like aerospace, automotive manufacturing, energy & power, and building environmental engineering.

### Strong Engagement and Positive Reception

According to ZWSOFT's official post-show report, the participation yielded significant results. The PHOENICS exhibit attracted **hundreds of professional visitors** for in-depth technical consultations. Preliminary cooperation intentions were established with **dozens of potential partners and leading industry enterprises** from around the globe, effectively boosting PHOENICS' international brand recognition and influence. The software's robust simulation capabilities, user-friendly interface, and efficiency in tackling complex engineering problems received high acclaim from attending experts and clients.

ZWSOFT's continued presence at Hannover Messe, a global industrial bellwether, underscores its commitment to the industrial software sector and strategic focus on international markets. PHOENICS' successful showcase not only reinforced its position as a premier professional CFD solution but also provided the global industrial community with a powerful tool for efficient and intelligent design exploration and optimization.

### Stay Updated on PHOENICS!

For further product information and upcoming event news, visit:

- PHOENICS Official Website: <https://www.cham.co.uk/>
- ZWSOFT WeChat Official Account: ZWSOFT\_Official

## CHAM Announces the Retirement of one of its Long-Standing Employees

*Jill Rayss<sup>a</sup> & Dr Mike Malin<sup>b</sup>*

*<sup>a</sup>Company Secretary, Concentration Heat and Momentum (CHAM)*

*<sup>b</sup>Technical Support Manager, Concentration Heat and Momentum (CHAM)*



Dr. John Ludwig, who joined CHAM in 1978, has walked through our entrance door many times during the last 46 years. He has held many positions, met many members of staff, and clients, and been located on almost every floor of the building.

1978 was the pre-PHOENICS era, and well before the term CFD entered common usage. During this long tenure, John has made profound and memorable contributions to all areas of the business.

Apart from being the target person for all things PHOENICS, John has managed the consultancy, development and user support teams. Also, as Software Services Manager, John was for a time responsible for delivering training courses and providing technical support to the sales team.

It goes without saying that John is in the 'CHAM Hall of Fame', but we must mention his tremendous contribution to the development of PHOENICS itself. This cements John's place in the "Holy Trinity" of PHOENICS developers. Of course, John already has legendary status for being the only person who ever managed to change Professor Brian Spalding's mind about a PHOENICS Development.

CHAM thanks you John for everything that you have done. We are sad to see you leave us as a member of staff. It has been a privilege to work with you and we wish you all the best in your retirement.

But, that is not the end of the story. John may no longer be an employee, but has agreed to continue to work with us temporarily as an external consultant, so he can pass on to others his expertise, and continue with his invaluable work, for which CHAM thanks you again.

The above is a picture taken in December 2024, of John's 'supposed' last day in the office, with Dr. Mike Malin, delivering the retirement speech.

### Contact Us:

CHAM's highly skilled, and helpful, technical team can assist in solving your CFD problems via proven, cost-effective, and reliable, CFD software solutions, training, technical support and consulting services. If YOU have a CFD problem why not get in touch to see how WE can help with the solutions?

See us on social media sites shown below:

